Integrating PCM into hollow brick walls: Toward energy conservation in Mediterranean regions

Youssef Hamidi, Zakaria Aketouane, Mustapha Malha, Denis Bruneau, Abdellah Bah, Rémy Goiffon

Version of Record: https://www.sciencedirect.com/science/article/pii/S0378778821004989
Manuscript_8700c6aebdbfd097fbdce91bd0c8ad8b

Integrating PCM into hollow brick walls: toward energy conservation in Mediterranean regions

Youssef HAMIDI[1*], Zakaria AKETOUANE[2, 3], Mustapha MALHA[1], Denis BRUNEAU[2, 3], Abdellah BAH[1], Rémy Goiffon[3]

[1] ERTE, Centre de Recherche en Energie, ENSET, Mohammed V University in Rabat, Morocco

[2] University of Bordeaux, CNRS, Arts et Metiers Institute of Technology, Bordeaux INP, INRAE, I2M Bordeaux, F-33400 Talence, France

[3] GRECCAU, EA 7482, ENSAP de Bordeaux, Talence, F-33400, France.

***Corresponding Author:** youssef.hamidi@um5s.net.ma

Abstract

Nowadays, cooling demand in the building sector is increasing in cooling-dominant climates because of extreme heat waves reinforced by climate change. As the demand for thermal comfort in buildings continues to grow, energy consumption increases accordingly. The application of phase change materials (PCM) to building envelopes can improve thermal energy storage, thus they can be used to increase the thermal mass of buildings. This article shows the efficiency of using PCMs to mitigate building cooling demands in eight cities representing the Mediterranean region: Al Hoceima (Morocco), Malaga (Spain), Marseille (France), Taher (Algeria), Naples (Italy), Tripoli (Libya), Ankara (Turkey), and Port Said (Egypt). The energy performance of three types of building: single-family, collective housing and hotel housing, built with hollow bricks, with and without PCMs, is evaluated in these cities using a numerical model based on the apparent heat capacity. A wide range of PCM melting temperatures is studied (from 22°C to 32°C). The results confirm that climate profoundly influences the storage/release process of PCMs. Regardless of the building typology, energy savings can reach 56% in the North-East Mediterranean cities using a PCM with a 26°C melting temperature, while no energy savings have been noted for the South-East cities. Finally, a correlation between the energy savings and the Cooling Degree Day is demonstrated, resulting in the recommendation of a PCM with a 26°C median melting temperature in a given location.

Keywords: Phase change materials, Low-energy Buildings, Energy-savings in buildings, Cooling needs reduction.

List of symbols

A : Area [m²]
C_p : Specific heat capacity [J/kg.K]
e : Energy [kWh/m²]
E : Energy [kWh]
F : Floor
g : Heat flux [W/m²]
h_r : radiative exchange coefficient
h : Height of holes [cm]
h_i : Inside convective heat transfer coefficient [W/m².K]
h_o : Outside convective heat transfer coefficient [W/m².K]
H : Height of hollow brick [cm]
J_i : Radiosity of the i^{th} surface [W/m²]
k : Thermal conductivity [W/m.K]
l : Length of holes [cm]
L : Length of hollow brick [cm]
L_f : Latent heat of fusion [kJ/kg]
q_s : Solar radiation [W/m²]
T : Temperature [K]
T_m : Median melting temperature [K]
T_{sky} : Sky temperature [K]
ΔE : Energy savings (%)
W_r : Window-to-wall ratio

max : Peak value
S : South orientation
E : East orientation
W : West orientation/west node
N : North
h : horizontal orientation
a : Air
pcm : Phase Change Material
b : Brick
o : Outdoor
i : Indoor, or incoming
l : Liquid state
s : Solid-state
α : Solar absorptivity
α_m : Solid PCM mass fraction
ε : Emissivity of surface
φ : Heat flux density [W/m²]
Φ : Heat flux [W]
ρ : Density |kg/m3]
σ : Stefan's constant
θ : Solid PCM volume fraction
h : Enthalpy
P : Surface proportion

1 Introduction

In this century, the world is experiencing energy transition guided mainly by the use of renewable energies and smart technologies. The main objective is to address greenhouse gas emissions and to significantly reduce the use of fossil fuels. The rapid increase in energy prices and recent geopolitical events serves as a notice of the importance of this energy transition for economic growth and human development, as well as the vulnerability of the global energy system in the face of shortages [1].

The building sector is considered as one of the largest energy-consuming sectors and equally responsible for carbon dioxide (CO_2) emissions [2]. Since 2010, global building-related CO_2 emissions and electricity consumption have risen continuously at an average rate of 1% and 2.5% per year, respectively [3]. Residential and commercial buildings consume more than one-third of the world's final energy. In some regions that depend strongly on biomass, energy consumption is as high as 80% [2].

As part of the energy transition, Smart home technologies and Responsive building envelopes represent a promising solution to reduce consumption by buildings by managing energy flows in terms of production, storage and use, while assuring comfort for the occupants [4]. The building envelope has an enormous impact on the need for space cooling; it is the main element separating the building's indoor and outdoor environments. It manages energy exchanges and regulates the storage capacity of the building. The selection of materials is of particular importance. Thermal mass is essential for space cooling, as it holds temperature longer and creates a natural barrier between indoor and outside temperatures, enhancing thermal comfort [5]. Traditional buildings with thick earthen or stone walls in light colors, such as those in relatively hot Mediterranean and North African climates, rarely need to be cooled mechanically [6]. However, in recent years, more heatwaves have been observed in these regions due to climate change. According to Alpert et al. [7], an increase in average surface temperatures in the Mediterranean region of between 3 and 5°C has been predicted for the period 2071-2100. This will have a direct influence on the rate of air conditioning systems installed and on energy consumption in the building sector in general.

One of the promising solutions in reducing cooling needs in buildings is the use of Phase Change Materials (PCM) [8], [9]; these materials can store thermal energy in the form of latent heat, and can be incorporated into active (Solar systems [10], HVAC systems [11], [12], etc.) and passive (building envelope [13]) solutions. Of all the applications of PCM in buildings, the most impressive is their incorporation into building materials to develop their thermal properties because of their high storage capacity [14]. The incorporation of PCM into building elements such as blocks, concrete, bricks, gypsum boards, mortars, and other materials has been studied [15]. PCM can be incorporated into walls, floors, or ceilings. Detailed descriptions of the latest studies are presented in Table 1.

Table 1. Summary of studies dealing with the integration of PCM into the building envelope

Study	Study Type	localization	Solution	PCM incorporation technique	PCM melting temperature	Main Results
Ručevskis et al. [16]	Numerical	Ceiling	Metallic panels	Macroencapsulation (Hybrid solution)	22°C	Indoor air temperature reduction by an average of 9.5°C during the analysis period, under Baltic States climatic conditions.
Maleki et al. [17]	Experimental	Wall & Ceiling	Gypsum Boards	Nanoencapsulation	24.93°C & 24.62°C	Reduction of indoor air temperature fluctuations and maintenance of thermal comfort for most of the year.
Kenzhekhanov et al. [18]	Numerical	Wall & Roof	Panels	Macroencapsulation	19°C to 27°C with 1°C increments	PCM23 and 24 have proven to be the best in terms of energy savings in the subarctic climate, with a payback period of 16 to 32 years, and 4817 kg/years CO_2 savings.
Kishore et al. [19]	Numerical	Wall	Panels	Macroencapsulation	12°C to 32°C with 2°C increments	PCM22 and 24 have been chosen as the optimum for reducing heat gain, and loss in various cities studied in the United States, but they are ineffective during the heating season.
Rathore et al. [20]	Experimental	Wall & Roof	Tubes	Macroencapsulation	37°C	Reduction of 27.32% in heat flux peak, 38.76% in cooling load leading to 0.4 US $/day for 1.12m*1.12m*1.12m cubicles in Mathura (India) climatic conditions.
Saxena et al. [21]	Experimental	Wall	Brick	Macroencapsulation	35°C & 33.6°C	Temperature reduction up to 9.5°C, and heat gain reduction of up to 60%.
Arıcı et al. [22]	Numerical	Wall	Panels	Macroencapsulation	-10°C to 40°C with 1°C increments	Maximum energy savings obtained by placing PCM in the interior side, and the annual optimum PCM melting temperature and its thickness depending on the studied cities.
Tunçbilek et al. [23]	Numerical	Wall	Panels	Macroencapsulation	20°C to 30°C with 1°C increments	Locating the PCM near the exterior increased the energy demand, up to 12.8% seasonal energy saving was attained with 23 mm of PCM25.
Bhamare et al. [24]	Numerical	Roof	Panels	Macroencapsulation	28°C	Ceiling temperature almost constant (between 25.5 and 27.5°C), and reduction in thermal load peak compared to a roof without PCM.
Cabeza et al. [25]	Experimental	Wall & Roof	Concrete	Microencapsulation	26°C	After ten years, the cabin with PCM has the same thermal response as that achieved in 2005, with no degradation of the thermal response of the PCM.
Yu et al. [26]	Numerical	Wall, Floor & Roof	Panels	Macroencapsulation	29°C	Due to the night heating effect, PCM29 is not adapted to the climate and the residential buildings in Hong Kong.
Fořt et al. [27]	Numerical	Wall	Gypsum Boards	Microencapsulation	24.68°C,24.91°C & 25.86°C	Energy savings range between 6 and 12%, and an improvement of 20% in interior heat recuperation.
Lu et al. [28]	Experimental	Ceiling	Ceiling	Shape-stabilization	31°C	Decrease the internal peak temperature by 2.1°C and 2.7°C under 8h and 12h timed cold storage strategy, respectively.

Applications to walls have received a great deal of interest in the scientific community [15]; this can be explained by the fact that the walls represent the largest surface area in the building. Cabeza et al. [29] monitored the behavior of concrete test cells with and without 5% of PCM microcapsules. Concrete with PCM incorporation was used in the roof, and the West and South walls. During the summer, they observed a difference of about 3°C on the West wall, on the maximum temperature surface. The same observation was made in another experimental study carried out by Castell et al. [30] of alveolar and conventional bricks with and without encapsulated PCM. A heat pump was used to set and control the inside temperature of the test cells. The results showed that during summer, electricity consumption was reduced by 15% in the compartments with PCM, resulting in around 1 to 1.5 kg/year/m^2 reduction in CO_2 emissions. Saxena et al. [31] examined the impact of PCM incorporation in bricks for Delhi climatic conditions in which two different PCMs (Eicosane and OM35) were evaluated. The results show a decrease in the indoor temperature between 4.5℃ and 7℃ during the peak hours of the day, an 8% and 12% decrease in heat flow using Eicosane and OM35, respectively. Gypsum boards are also used in walls as a lining element, which guarantees that most areas of the room can be used. Shilei et al. [32] conducted studies on test cells with a 9.5 mm thick gypsum wallboard containing 26% PCM, with a transition temperature between 17.9°C and 20.3°C. The investigation was able to verify a lower temperature oscillation in the test rooms coated with PCM gypsum boards. After one year, Shilei et al. [33] developed gypsum boards with PCM to be applied to the wall surface to decrease the cooling load in a test cell. Compared with a standard room, it was found that the PCM wallboard room could significantly reduce HVAC systems energy costs. In order to assess the effect of the design of the PCM gypsum board for thermal effectiveness, Darkwa et al. [34] investigated the behavior of randomly mixed and laminated PCM drywalls. The results confirmed that the use of laminated PCM is more practical since it contributes to the increase in thermal inertia.

Various authors have studied building fabric solutions incorporating PCMs into the roof or ceiling [35]–[40]. For example, Pasupathy et al. [37] evaluated the influence of a 2.5 cm PCM panel located on the roof between two slabs, the lower one formed of concrete and the upper one composed of brick and mortar. A difference of 3°C in the maximum surface temperature was recorded. Chou et al. [41] developed new metallic roofing with PCM to adapt its thermal performance to the thermal comfort of the interior space. The results showed that the new design helped to control the indoor air temperature better by shifting and reducing the peak temperature of the room. Other solutions were also developed regarding the

ceiling panels with capillary networks for PCM circulation; for instance, Griffiths et al. [35] used a microencapsulated PCM with a transition temperature of 18°C in aqueous suspension, for use in a chilled ceiling system. The data collected showed that a 40% concentration of PCM in aqueous suspension could be useful as a heat transfer fluid in a chilled ceiling application.

The application of solutions with PCM on the floor has also been an area of study by several researchers such as X. Jin et al., S. Lu et al., K. Lin et al., K. Nagano et al., and A. G. Entrop et al. [42]–[46]. Nagano et al. [45] developed a system with PCM incorporation in the floor. The system consisted of a granular latent heat storage material made from foamed glass beads with paraffin wax and then applying three layers of urethane. The results showed that the PCM phase change occurred between 17°C to 22°C, with 31 kJ/kg enthalpy. In this way, it was possible to keep the indoor temperature between 1.5-2.1 times longer against a reference solution, as well as daily energy storage of 1.79 MJ/m^2.

The envelope constructed with hollow brick walls and roofs incorporating phase-change materials (PCM) has a vital impact on the amount of heat entering a building and, therefore on the need for mechanical cooling. This work is a continuation of our earlier study [47] in which significant energy savings were reported during summer in six weather zones in Morocco. In this work, the study area has been extended to cover the entire Mediterranean region, represented by eight cities: Al Hoceima (Morocco), Malaga (Spain), Marseille (France), Taher (Algeria), Naples (Italy), Tripoli (Libya), Ankara (Turkey), and Port Said (Egypt). The integration of a wide variety of PCMs into hollow bricks (see Fig.1) with melting temperatures ranging from 22°C to 32°C is investigated in order to:

- compare the thermal performance of the hollow bricks when using various PCMs and when they contain only air, by analyzing the heat flow density
- evaluate the energy savings in the eight cities considered
- determine conditions that allow (or not) the use of the appropriate PCM based on the Cooling Degree Day

Figure 1. Hollow brick - eight holes

2 Methodology

2.1 Problem statement

2.1.1 Geometry of hollow brick

In this research, a standard building envelope is studied. It consists of a wall of hollow bricks each with eight holes (Fig.1). The geometry of these earthenware bricks is shown in Fig.2; they are L=6cm thick and H=15cm high and include eight rectangular holes l=2cm x h=2.5cm, which can be charged with PCM. The outside surface of the bricks is exposed to the regular variation of solar radiation and the convection of the external air. The inside surface of the bricks is subjected to the convection of indoor air at a constant temperature of 26°C.

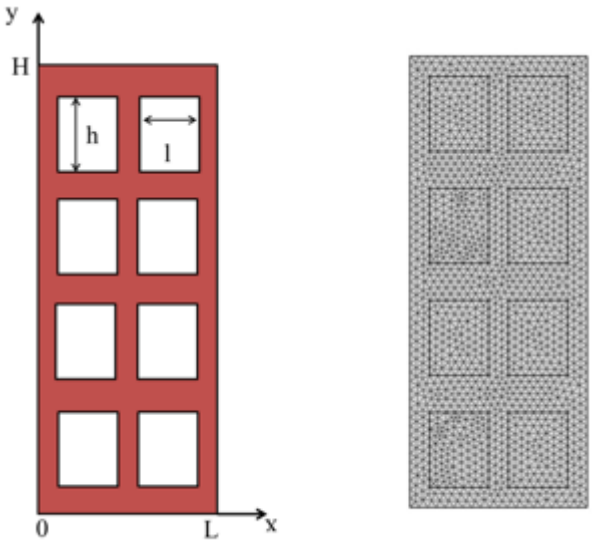

Figure 2. Schematic representation of hollow brick and triangular mesh generation of 3088 elements

Six PCMs are investigated, differing mainly in terms of median melting temperature T_m (from 22°C to 32°C). In addition, the PCMs considered in this study are organic PCM-type made of pure paraffin, especially the RT-Line (from Rubitherm) used between T_m=22°C and T_m=30°C. For T_m=32°C, we consider the fatty acid PCM-type Capric Acid ($C_{10}H_{20}O_2$). The thermophysical properties of PCMs and the brick used in this numerical study are presented in Table 2. From an experimental point of view, PCM can be inserted into the holes of the brick using plastic film containers or with insertion of metal steel macrocapsules as demonstrated by Vicente *et al.* [48] and Hichem *et al* [49]. This insertion allow to solving leakage problems of liquid PCM.

Table 2. Thermophysical properties of six PCMs and the brick

Material	**T_m(°C)**	**k (W/m.K)**		**C_p(kJ/kg.K)**		**ρ (kg/m3)**		**L_f (kJ/kg)**
		Solid	Liquid	Solid	Liquid	Solid	Liquid	
Brick	-	0.5	-	2.000	-	900	-	-
Paraffin RT22 [50]	22	0.2	0.2	2	2	760	700	190
Paraffin RT24 [50]	24	0.2	0.2	2	2	880	770	160
Paraffin RT26 [50]	26	0.2	0.2	2	2	880	750	180
Paraffin RT28 [50]	28	0.2	0.2	2	2	880	770	250
Paraffin RT30[50]	30	0.2	0.2	2	2	880	760	250
Capric Acid ($C_{10}H_{20}O_2$)[51]	32	0.149	0.149	2.096	2.088	1004	886	152

2.1.2 Governing equations

In this work, COMSOL Multiphysics software was used [52], in which a dynamic two dimensional (2D) model of heat transfer through the hollow brick is solved using the finite element method. Two configurations are studied in which the holes of the brick contain PCM or air. The time step (Δt) of simulation and mesh refinement influence, and the validation of the model, were carried out in our previous work [47]. Finally, simulations are performed with a triangular mesh of 3088 elements, time step of Δt=360s, and a value of 10^{-6} for the iteration convergence criterion.

To evaluate heat flux evolutions and temperatures inside our hollow brick, we considered the following hypotheses:

- Bricks have constant thermophysical properties;
- Bricks are dry (non-evaporative heat source);
- Contact between PCM/air and brick hole surfaces is ideal;

- No convection within the melted phase of PCM;
- Range of narrow-phase change temperature is 1°C;
- No thermal mass and ground radiation.

The heat transfer at the brick component (b index) verifies the next equation for brick temperature T_b:

$$\rho_b C_{p,b} \frac{\partial T_b}{\partial \mathrm{t}} = k_b \left(\frac{\partial^2 T_b}{\partial x^2} + \frac{\partial^2 T_b}{\partial y^2}\right) \quad (1)$$

In the PCM component, heat transfer (PCM index) is modeled using the energy balance equation, which considers the formulation of PCMs' apparent heat capacity[53]; this formulation assumes that the phase change occurs with a small temperature variation. The width value of this phase change temperature interval has only a small effect on the heat flux density exchange between PCMs and their environment, according to Thiele et al. 2015[54]; thus, in this work, a melting range of ΔT= 1K was chosen. Finally, in the PCM components, heat transfer can be described by the following governing equations [55]:

$$\rho_{pcm} C_{p,pcm} \frac{\partial T_{pcm}}{\partial \mathrm{t}} = k_{pcm} \left(\frac{\partial^2 T_{pcm}}{\partial x^2} + \frac{\partial^2 T_{pcm}}{\partial y^2}\right) \quad (2)$$

Where:

$$\rho_{pcm} = \theta\, \rho_s + (1-\theta)\rho_l \quad (3)$$

$$C_{p,pcm} = \frac{1}{\rho}\left(\theta\, \rho_s C_{p,s} + (1-\theta)\rho_l C_{p,l}\right) + L_f \frac{\partial \alpha_m}{\partial T} \quad (4)$$

$$k_{pcm} = \theta\, k_s + (1-\theta) k_l \quad (5)$$

In which, θ represents the solid volume fraction of PCMs, defined as follows:

$$\begin{cases} \theta = 1 & if\ T_{pcm} \le T_m - \dfrac{\Delta T}{2} \\ \theta = \dfrac{1}{\Delta T}\left(T_m + \dfrac{\Delta T}{2} - T_{pcm}\right) & if\ T_m - \dfrac{\Delta T}{2} \le T_{pcm} \le T_m + \dfrac{\Delta T}{2} \\ \theta = 0 & if\ T_{pcm} \ge T_m + \dfrac{\Delta T}{2} \end{cases} \quad (6)$$

Where: T_m represents the median melting temperature of the PCMs.

The solid PCM mass fraction α_m can then be expressed as follows:

$$\alpha_m = \frac{1}{2}\frac{(1-\theta)\rho_l - \theta\ \rho_s}{\theta\ \rho_s + (1-\theta)\ \rho_l}. \tag{7}$$

The equations of the air component (a index) are the Navier-Stokes equation and energy equation as follows:

$$r_a C_{p,a}\left(\frac{\partial T_a}{\partial t} + u\frac{\partial T_{a,x}}{\partial x} + v\frac{\partial T_{a,y}}{\partial y}\right) = k_a\left(\frac{\partial^2 T_{a,x}}{\partial x^2} + \frac{\partial^2 T_{a,y}}{\partial y^2}\right) \tag{8}$$

In addition, when considering the radiative exchanges between the inside surfaces of the brick holes, each hole surface exchanges with the other three surfaces, following the density of radiative heat flux obtained from Radiosity modeling:

$$q_{b,i} = G_{b,i} - J_{b,i} \tag{9}$$

Where: $J_{b,i} = (1-\varepsilon)\ G_{b,i} + \varepsilon\sigma T_{b,i}^4$ and $G_{b,i}$ represents the i-surface Radiosity and the incidence radiations on this surface, respectively.

2.1.3 Boundary conditions

The outside surface of the bricks receives solar radiation, which depends on the facade orientation and time of day, and the convective heat exchanges with the outdoor air, and also radiative heat exchange with the sky, only for the horizontal surface (roof). The following equation gives the incident heat flux density $\varphi_o(t)$ on the outside facades:

$$\varphi_o(t) = k_b\frac{\partial T_b(\mathrm{x=0,y,t})}{\partial \mathrm{x}} = \mathrm{h_o}\left(\mathrm{T_o} - \mathrm{T_b}(\mathrm{x}=0,\mathrm{y},\mathrm{t})\right) + \mathrm{h_r}\left(\mathrm{T_{sky}} - \mathrm{T_b}(\mathrm{x}=0,\mathrm{y},\mathrm{t})\right) + \alpha\ \mathrm{q_s}(t) \quad ,\forall y \in [0,H] \tag{10}$$

T_o represents the outdoor air temperature, T_{sky} is sky temperature and q_s represents the incident solar flux density received by the external surface of the bricks. α is the brick solar absorption coefficient (assumed to be α=0.6) [56], and h_o is the external convective heat transfer coefficient (assumed to be h_o =25 W/m².K) [57].

Moreover, h_r is the coefficient of radiative exchange with the sky, which can be expressed as:

$$h_r = \sigma\, \varepsilon_b\, (T_b(x = 0, y, t) + T_{sky})(T_b^2(x = 0, y, t) + T_{sky}^2) \quad (11)$$

Where σ is it Stefan's constant and ε_b=0.9 is emissivity in the infrared longwave radiation of the brick.

On the inside surface of the bricks, a convective boundary condition was applied and an indoor temperature set value of T_i=26°C (U.S. Department of Energy recommendation). The density of the heat flux coming from outside is given by:

$$\varphi_i(t) = -k_b \frac{\partial T_b(x = L, y, t)}{\partial x} = -h_i\big(T_i - T_b(x = L, y, t)\big) \qquad ,\forall y \in [0, H] \quad (12)$$

Where h_i represents the inside convective heat transfer coefficient, which depends on the heat flow direction (see Table 3) [57].

Table 3. Value of the inside heat transfer coefficient versus heat flow direction [57]

	Direction of heat flow		
	Upwards	Horizontal	Downwards
h_i (W/m².K)	10	7.69	5.88

Heat losses are disregarded on the bottom and the top faces of the wall brick:

$$-k_b \frac{\partial T_b(x, y = H, t)}{\partial y} = k_b \frac{\partial T_b(x, y = 0, t)}{\partial y} = 0 \qquad ,\forall x \in [0, L] \quad (13)$$

The brick containing PCM or air is assumed to have a uniform initial temperature:

$$\begin{cases} T_b\,(t = 0, x, y) = T_{pcm}\,(t = 0, x, y) = 25°C \quad ,\forall (x, y) \in \{[0, L];\ [0, H]\} \\ \text{or} \\ T_b\,(t = 0, x, y) = T_a\,(t = 0, x, y) = 25°C \quad ,\forall (x, y) \in \{[0, L];\ [0, H]\} \end{cases} \quad (14)$$

3 Results & discussion

This section evaluates the performance of the use of PCMs in the building envelope with the aim of guiding decision-makers in integrating the appropriate PCM in the Mediterranean region. To this end, the first part will present the representative cities selected for our study. In the second part, the density of heat flux through a wall will be analyzed for East, West, South, North orientations, and the roof on a typical summer day. In the third part, we will present the energy savings and the heat flux peak reduction indicators for three typical buildings that integrate each of the six PCMs considered in this study. Finally, recommendations for the use of the appropriate PCM depending on the Cooling Degree Day are discussed.

3.1 Meteorological data of Mediterranean cities

For the most part, the climatic conditions decide the PCM performance. For this reason, and in order to obtain an extended range of climate conditions, the study was carried out for eight Mediterranean climates: Al Hoceima (Morocco), Malaga (Spain), Marseille (France), Taher (Algeria), Naples (Italy), Tripoli (Libya), Ankara (Turkey), and Port Said (Egypt). The geolocation of each city is shown in Figure 3.

According to the Köppen-Geiger classification [58], Al Hoceima, Malaga, Marseille, Naples and Taher are characterized by a dry summer climate. Tripoli, Port Said, and Ankara climates are classified as hot semi-arid, desert, and humid continental, respectively. In order to illustrate the differences in climatic condition between the selected locations, we calculate the solar energy received by a horizontal surface and the Cooling Degree Days in each city using a baseline temperature of 21°C (see Table 4).

Figure 3. Geographical map of the Mediterranean region.

Table 4. Cooling Degree Days in the eight Mediterranean locations

City	Cooling Degree Day (CDD)	Solar energy (kWh/(m².year))
Malaga (Spain)	516	825
Al Hoceima (Morocco)	296	865
Marseille (France)	367	787
Taher (Algeria)	585	802
Naples (Italy)	429	768
Tripoli (Libya)	1101	873
Ankara (Turkey)	229	694
Port Said (Egypt)	953	876

3.2 Heat flux density analysis

In this part, the heat flux density at the inside surface of the bricks in the East, South, West, North, and horizontal orientations is considered. The simulations performed for PCM median melting temperatures of 22°C, 24°C, 26°C, 28°C, 30°C and 32°C suggest two leading climatic groups corresponding to two different main thermal behaviors concerning heat flux density:

- The North Mediterranean: where Malaga (Spain) and Marseille (France) are influenced by the oceanic climate, and the continental climate has influenced Naples (Italy) and Ankara (Turkey).

- The South Mediterranean: impacted by the arid climate, affecting Al Hoceima (Morocco), Taher (Algeria), Tripoli (Libya), Port Said (Egypt).

Here we show results for Tripoli (Libya) and Naples (Italy). Fig.4 presents the ambient temperature and solar radiation of these representative cities for a typical day in summer (i.e., July 21).

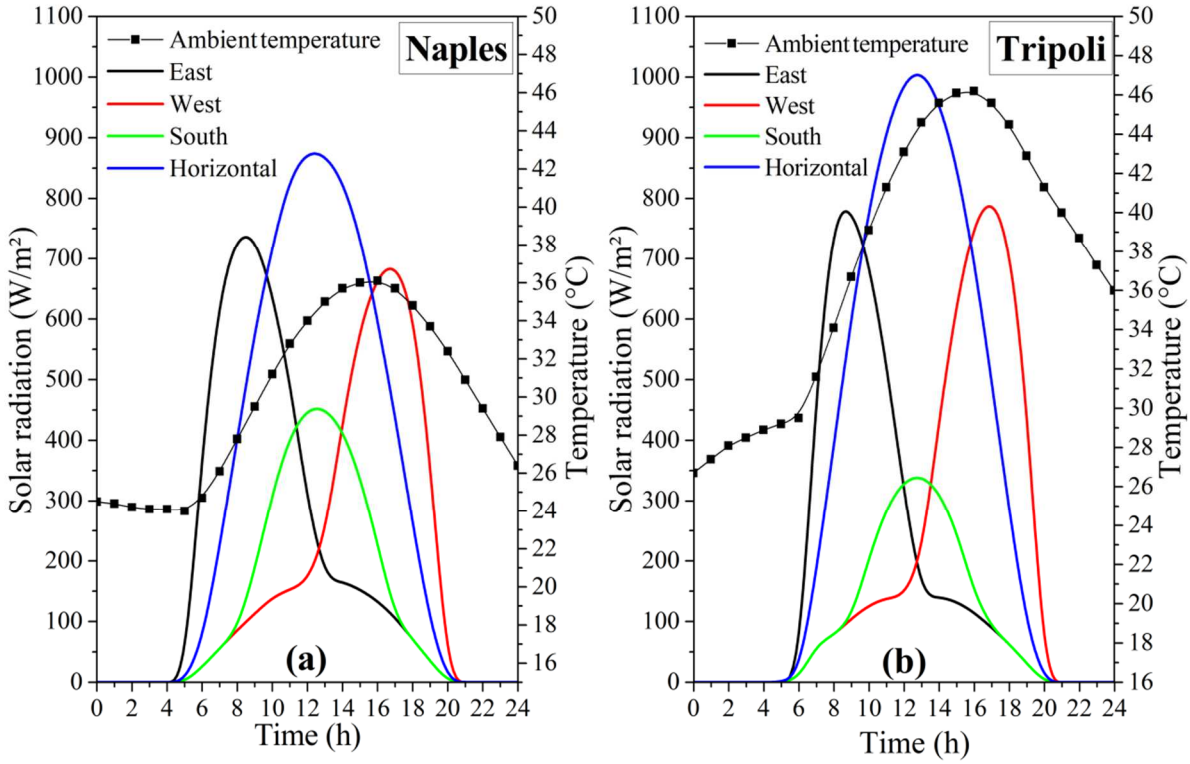

Figure 4. July 21 solar radiation on vertical (East, West, South, North) and horizontal surfaces, and outdoor air temperature in Naples (a) and Tripoli (b).

- East oriented wall

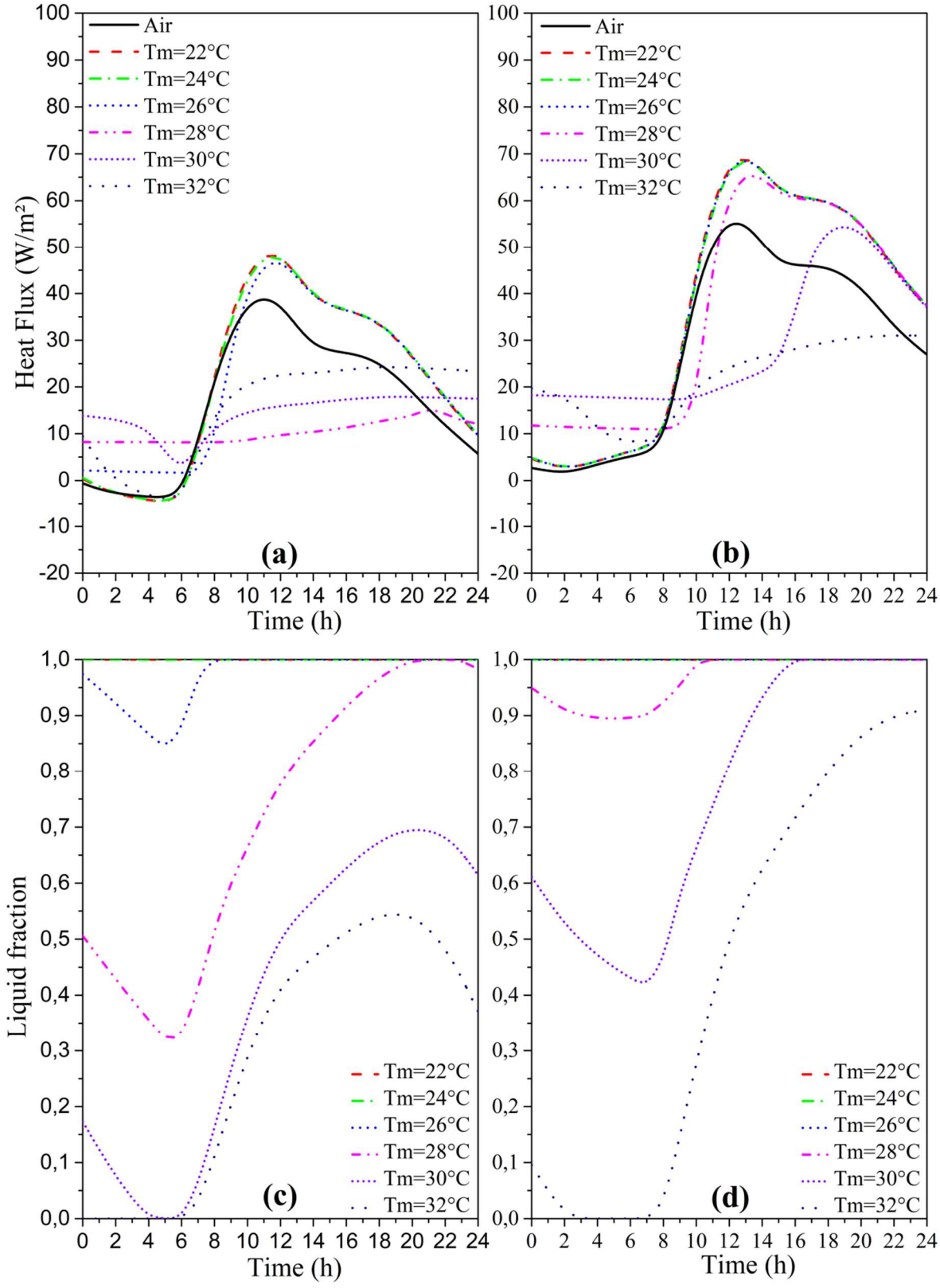

Figure 5. (a) and (b): Heat flux density at the internal surface of the bricks with Air or PCM for East wall orientation, in Naples and Tripoli respectively. (c) and (d): Liquid fraction of the PCM in the holes of the hollow brick, Naples and Tripoli respectively

Fig. 5 shows incoming heat flux density $\varphi_i(t)$ (towards interior) at the inside surface of the East-facing wall in Naples (a) and Tripoli (b), for a hollow brick charged with air and hollow bricks charged with six PCMs with median melting temperatures Tm=22°C (dashed line), Tm=24°C (dotted-dashed-dotted line), Tm=26°C (Short dashed line), Tm=28°C (dashed-dotted-dotted line), Tm=26°C (short dotted line) and Tm=32°C (dotted line). Corresponding PCM liquid fraction 1-θ(t) is also reported in Fig.5-(c) for Naples and Fig.5-(d) in Tripoli. These figures give rise to some critical comments (see Table 5).

Table 5. Elemental analysis of heat flux density and liquid fraction variations for the 6 PCMs used in Naples and Tripoli climates.

PCM	City	Time interval	Heat flux density variations $\varphi_i(t)$	Liquid fraction variations
T_m=22°C	Naples	[12:00 AM; 12:00 AM]	follows variations of external conditions	1-θ=1
	Tripoli	[12:00 AM; 12:00 AM]	follows variations of external conditions	1-θ=1
T_m=24°C	Naples	[12:00 AM; 12:00 AM]	follows variations of external conditions	1-θ=1
	Tripoli	[12:00 AM; 12:00 AM]	follows variations of external conditions	1-θ=1
T_m=26°C	Naples	[12:00 AM; 03:00 AM]	constant and positive	1-θ decreases
		[03:00 AM; 07:00 AM]	constant and positive	1-θ increases
		[07:00 AM; 12:00 AM]	follows variations of external conditions	1-θ=1
	Tripoli	[12:00 AM; 12:00 AM]	follows variations of external conditions	1-θ=1
T_m=28°C	Naples	[12:00 AM; 06:30 AM]	constant and positive	1-θ decreases
		[06:30 AM; 07:00 PM]	constant and positive	1-θ increases
		[07:00 PM; 12:00 AM]	follows variations of external conditions	1-θ=1
	Tripoli	[12:00 AM; 06:00 AM]	constant and positive	1-θ decreases
		[06:00 AM; 10:00 AM]	constant and positive	1-θ increases
		[10:00 AM; 24:00 AM]	follows variations of external conditions	1-θ=1
T_m=30°C	Naples	[12:00 AM; 04:30 AM]	constant and positive	1-θ decreases
		[04:30 AM; 06:00 AM]	follows variations of external conditions	1-θ=0
		[06:00 AM; 12:00 AM]	constant and positive	1-θ increases
	Tripoli	[12:00 AM; 06:00 AM]	constant and positive	1-θ decreases
		[06:00 AM; 03:30 PM]	constant and positive	1-θ increases
		[03:30 PM; 12:00 AM]	follows variations of external conditions	1-θ=1
T_m=32°C	Naples	[12:00 AM; 06:00 AM]	follows variations of external conditions	1-θ=0
		[06:00 AM; 10:00 AM]	follows variations of external conditions	1-θ increases
		[10:00 AM; 08:00 PM]	constant and positive	1-θ increases
		[08:00 PM; 12:00 AM]	constant and positive	1-θ decreases
	Tripoli	[12:00 AM; 03:00 AM]	follows variations of external conditions	1-θ decreases
		[03:00 AM; 07:30 AM]	follows variations of external conditions	1-θ=0
		[07:30 AM; 10:00 AM]	follows variations of external conditions	1-θ increases
		[10:00 AM; 12:00 AM]	constant and positive	1-θ increases

Comprehensively, direct observations can be interpreted as follows:

- When the PCM is partially liquid (partially solid), this is when it can accumulate or restitute latent heat; the heat flux density at the inside surface of the wall is constant and negative (outgoing), or constant and positive (incoming), or follows variations in external conditions approximately with a thermal phase shift and a small amplitude in comparison to the hollow brick with air.

- When PCM is fully solidified or melted, outdoor conditions impose the heat flux density at the inside surface of the wall with a time-delay due to the thermal wall mass; in this case, the direction of heat transfer by conduction in the brick depends on boundary conditions on its inside and outside surfaces.

For PCM median melting temperatures of Tm=22°C, 24°C in Naples and Tm=22°C, 24°C, 26°C in Tripoli, the heat flux density at the inside surface of the wall is forced by external conditions during the entire day. The median melting temperature of both these PCMs is too low, and they remain in100% liquid states during this period; therefore, latent heat storage is not used. We can also note that the peak of the heat flux density using these two PCMs is higher than that of the brick with air. This can be explained by the thermal conductivity of the PCM, which is higher than the air. Finally, we can observe that three PCMs (T_m=28°C, T_m=30°C, and T_m=32°C) in Naples and only one PCM (T_m=32°C) in Tripoli can reduce the peak of the heat flux density.

- South oriented wall

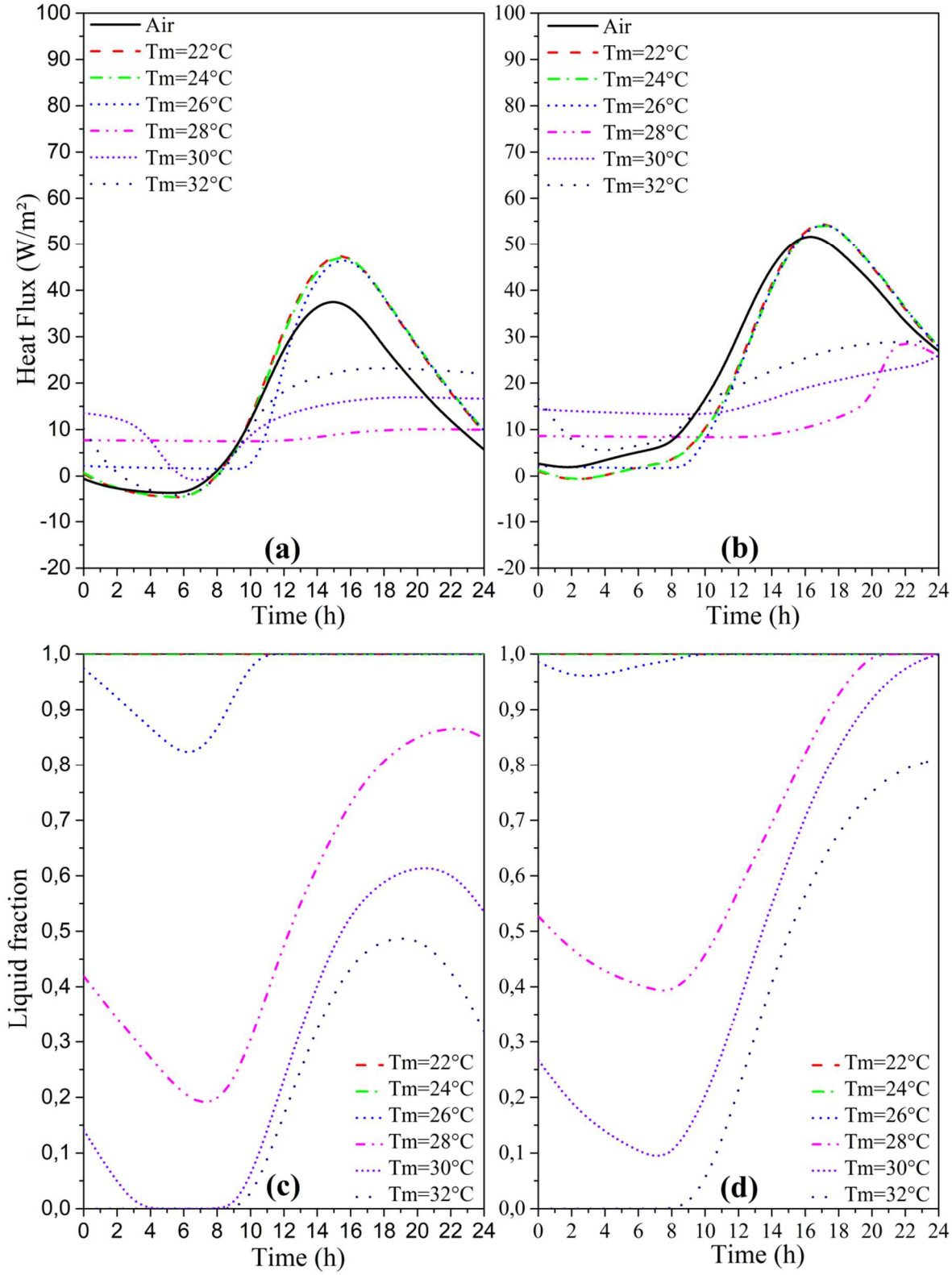

Figure 6. (a) and (b): Heat flux density at the internal surface of the hollow bricks with air or PCM for South wall orientation, in Naples and Tripoli respectively. (c) and (d):Liquid fraction of the PCM in the holes of the hollow brick, Naples and Tripoli respectively

Fig. 6 represents the results of the South-facing wall in Naples and Tripoli. Similar behaviors can be observed concerning heat flux density and PCM state when compared with East-facing wall results (see Fig. 5). The principal difference between the East-facing and South-facing walls is the time of day of the heat flux density peak: it occurs during the morning for East-facing and early in the afternoon for South-facing, mainly as a consequence of the solar radiation peak time in both orientations (see Fig. 4).

Note also that the heat flux density peak for the East-facing wall is slightly higher than for the South-facing wall for hollow brick filled with Air/PCM in Tripoli. This is because of the high value of the Normal incident component of the direct solar radiation received by the East-facing wall compared to the South-facing wall.

- West oriented wall

Fig.7 deals with the West-facing wall in Naples and Tripoli, where similar thermal behaviors to the East-facing and South-facing walls can be observed. Heat flux density peak and PCM state peaks are around 6 p.m. because of solar radiation. Moreover, heat flux density peaks in Naples for PCM median melting temperatures of T_m=30°C and 32°C, and in Tripoli for PCM median melting temperature of T_m=32°C were reduced and for the most part did not deviate from those observed for East-facing and South-facing walls for the same PCM. For this same day (i.e., July 21), these two PCMs are fully efficient respectively in Naples and Tripoli to limit the heat flux density indoors via vertical walls throughout the daytime.

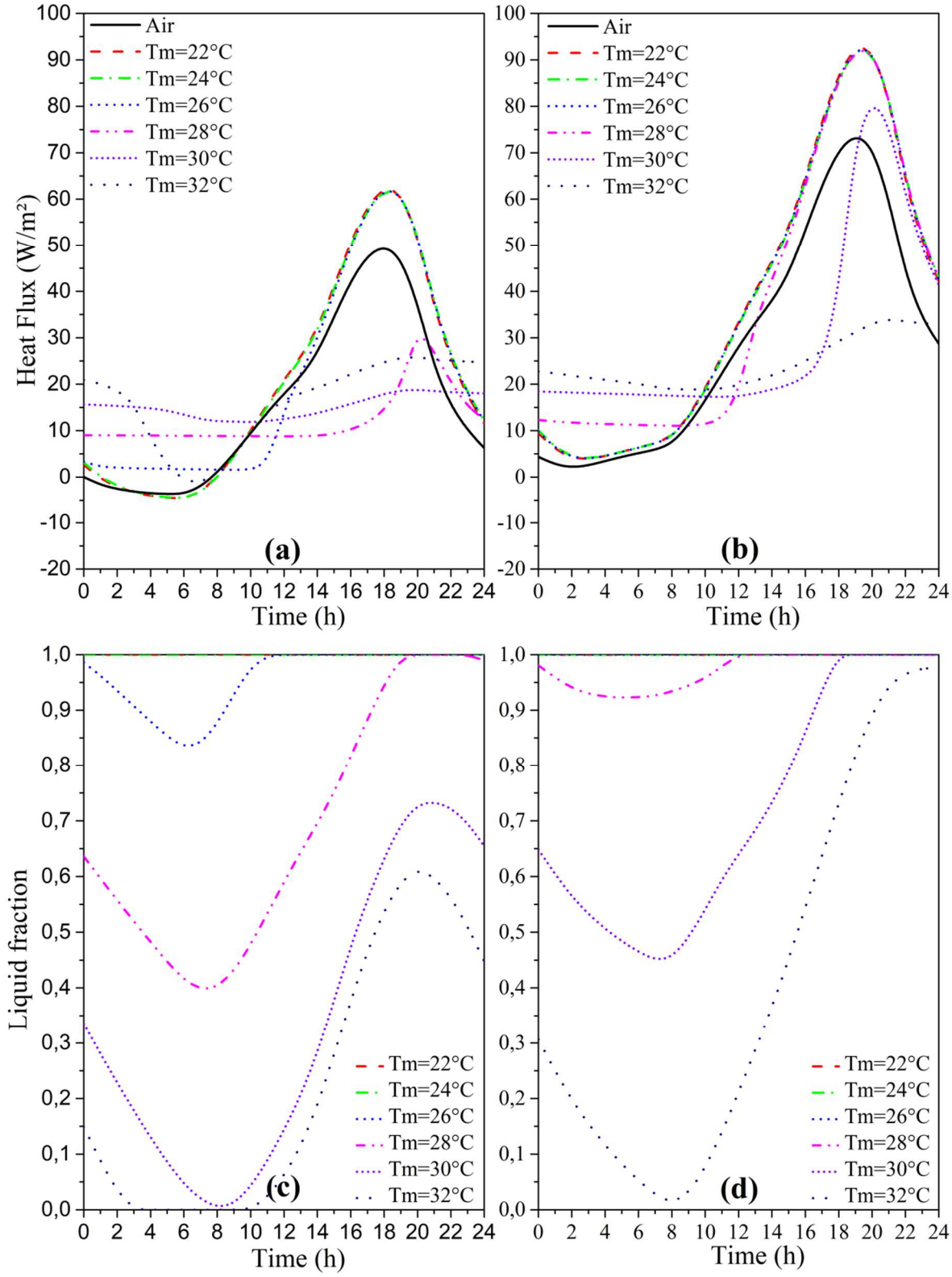

Figure 7. (a) and (b): Heat flux density at the internal surface of the bricks with air or PCM for West wall orientation, in Naples and Tripoli respectively. (c) and (d): Liquid fraction of the PCM in the holes of the hollow brick, Naples and Tripoli respectively

- North oriented wall

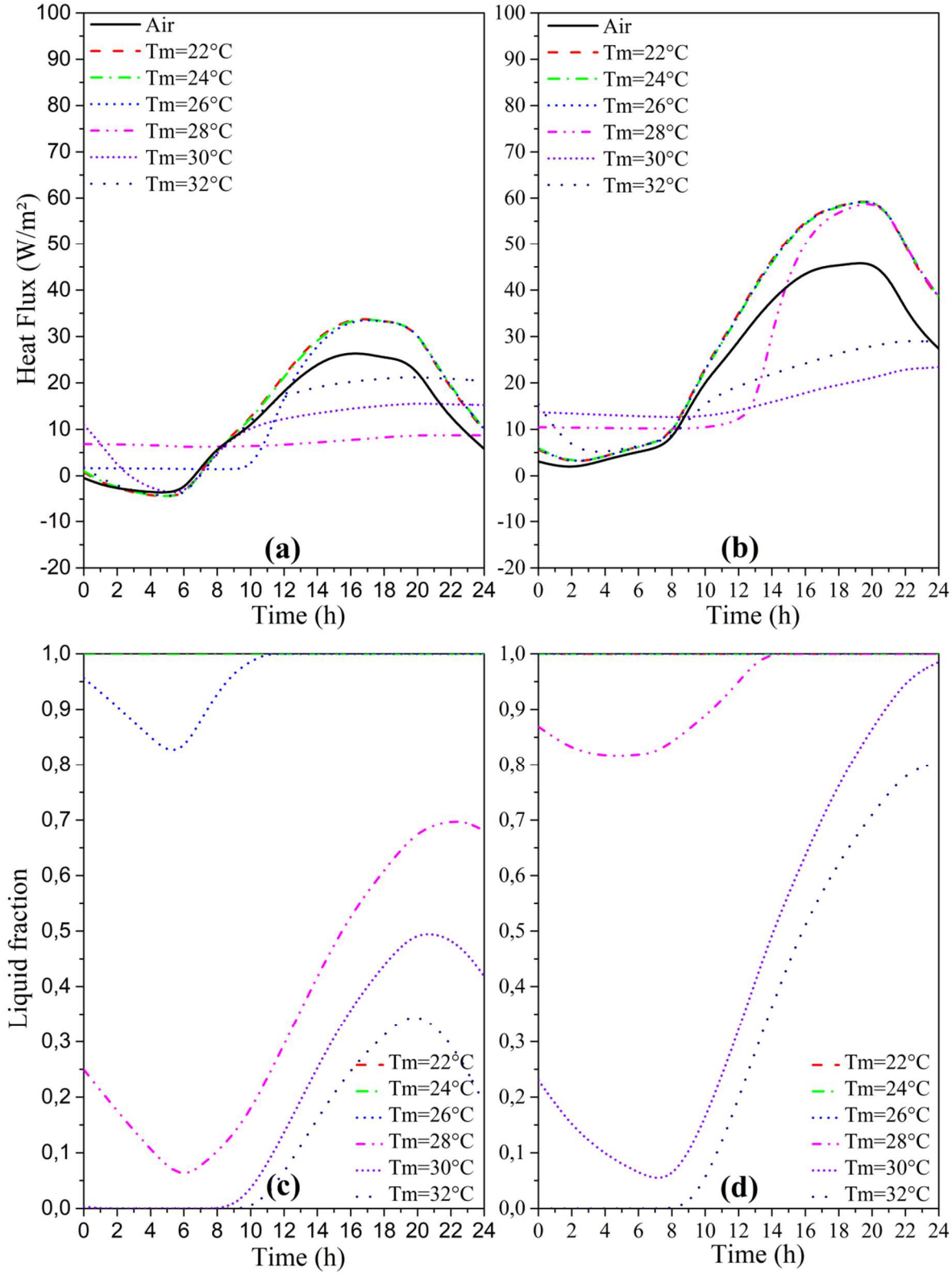

Figure 8. (a) and (b): Heat flux density at the internal surface of the bricks with air or PCM for North wall orientation, in Naples and Tripoli respectively. (c) and (d): Liquid fraction of the PCM in the holes of the hollow brick, Naples and Tripoli respectively

Fig. 8 concerns the North-facing wall in Naples and Tripoli. One can observe that the heat flux density, in addition to the PCM state, has a similar behavior to those observed for the East, South, and West-facing walls. However, the maximum heat flux density value for the North-facing wall is less than that for other orientations in Naples and Tripoli: the incoming heat flux is mostly due to the external air convection since direct solar radiation is negligible.

As regards heat flux peak reduction, the PCM with Tm=28°C, 30°C, and 32°C median melting temperature are efficient in Naples, while the PCM with Tm=30°C and 32°C median melting temperature is more useful in Tripoli. The other PCMs with Tm=22°C, Tm=24°C, and Tm=26°C median melting temperatures cause no reduction in Naples compared to the hollow brick with air. The same results are obtained in Tripoli for PCM with Tm=22°C, Tm=24°C, Tm=26°C, and Tm=28°C median melting temperatures.

- Horizontal oriented wall

Fig. 9 is about the horizontal orientation (i.e., roof) in Naples and Tripoli. The horizontal orientation could be considered in terms of direct solar radiation as a weighted sum of the East, South, and West orientations.

PCMs with T_m=28°C and T_m=32°C median melting temperatures, in Naples and Tripoli respectively, are efficient in limiting the heat flux density because the PCM partially melts during the daytime. In Tripoli, irrespective of the PCM median melting temperature value, it can be noticed that the heat flux density is positive throughout the daytime and nighttime. The external temperature is always higher than the set point temperature value (26°C), which means that heat flux density will always enter the room during July 21.

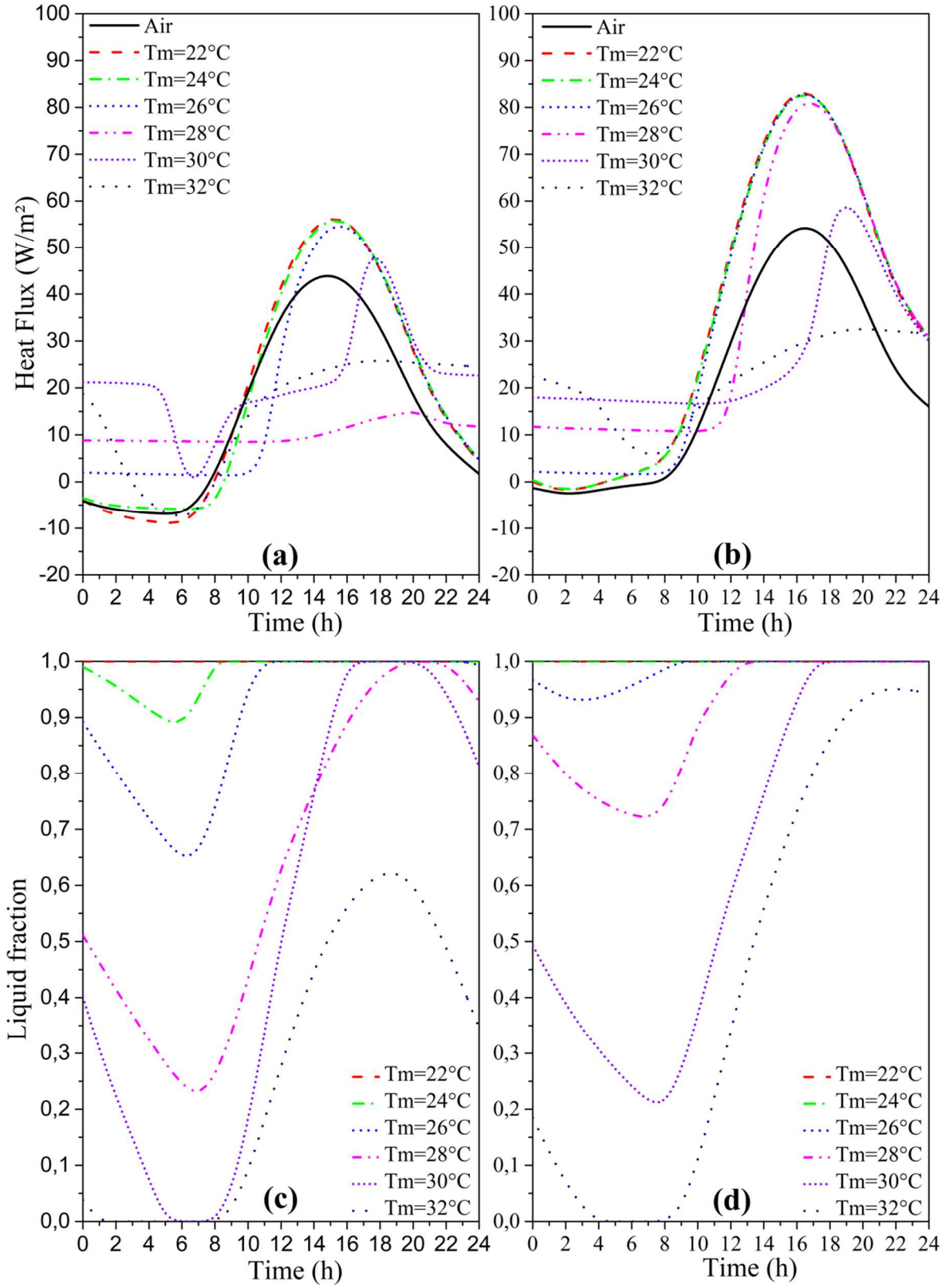

Figure 9. (a) and (b): Heat flux density at the internal surface of the bricks with air or PCM for horizontal wall orientation, in Naples and Tripoli respectively. (c) and (d): Liquid fraction of the PCM in the holes of the hollow brick, Naples and Tripoli respectively

3.3 Energy Saving Potential in the Mediterranean Region

After analysing the performance of the use of PCMs in the building envelope, we will examine the potential for energy savings and for reducing peak cooling demand during the summer for three types of building: single-family housing, collective housing, and hotel housing. Finally, we will deduce the values of the melting temperature range that can lead to energy savings in buildings located in the Mediterranean region.

3.3.1 Typology of the selected buildings

Three architectural models corresponding to three typical buildings are initially defined in terms of geometry; these are single-family, collective, and hotel housing. These dwellings are respectively two-floor (2F), five-floor (5F), and fifteen-floor (15F) buildings with each floor three meters high. Fig. 10 shows a 3D Building Sketch for these three building types.

From this architectural modeling, the proportions of the opaque surface for all types of wall (East wall "E"; South wall "S"; West wall "W"; North wall "N"; horizontal wall "h") can be determined (see Table 6). The proportion of window area per facade is considered similar for all the cases studied; it is represented by the window-to-wall ratio noted W_r. Since this study focuses on the heat gains through the opaque elements of the building, the Window-to-wall ratio is then taken as W_r=0%. Moreover, the equations described in the following sections give the possibility of considering other values of W_r.

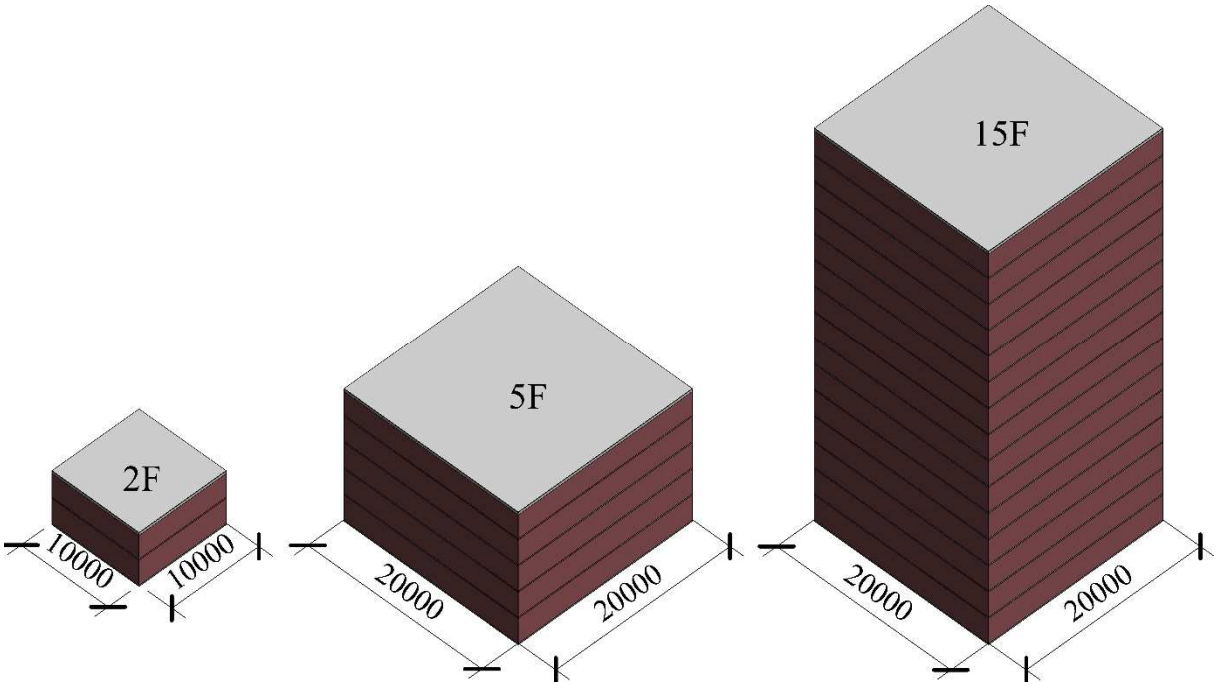

Figure 10.3D Building sketch of the three housing types

Table 6. Surface proportion of all wall orientation for three building types

Housing types	**Surface proportion**				
	$\mathbf{P_E}$	$\mathbf{P_S}$	$\mathbf{P_W}$	$\mathbf{P_N}$	$\mathbf{P_h}$
2F	0.18	0.18	0.18	0.18	0.29
5F	0.19	0.19	0.19	0.19	0.25
15F	0.23	0.23	0.23	0.23	0.10

3.3.2 Energy savings evaluation

To estimate the efficiency of incorporating PCMs into hollow bricks in buildings, two criteria were examined. The first is the energy savings that could be obtained by using these PCMs during the summer (21 May-15 September). The second concerns the estimate of heat flux peak reduction during summer. From these two criteria the energy needs and the cooling system power can be calculated.

The incoming heat flux density peak $\varphi_{i,\cdot}^{max,*}$ through each type of wall and windows (solar flux density), the incoming energy density through the walls $e_{\cdot}^{*}$ and solar energy density through the windows e_s^* during the summer can be obtained as follows:

$$\varphi_{i,\cdot}^{max,*} = \max[P_* \varphi_i^*(t) + W_{r,*}\ \tau\ q_s^*(t)] \quad (15)$$

$$e_s^* = \int \tau \, q_s^* \, dt \tag{16}$$

$$e_\cdot^* = \int g(t) \, dt \tag{17}$$

where
$$\begin{cases} g(t) = \varphi_i^*(t) & \varphi_i^*(t) > 0 \\ g(t) = 0 & \varphi_i^*(t) < 0 \end{cases}. \tag{18}$$

where τ is the solar transmittance of the windows.

In the below equations, • represents PCM or air, depending on what fills the holes in the bricks, and * is the wall orientation E, S, N, W, or H, corresponding to East, South, North, West and horizontal orientations.

These simulation results also enable us to calculate the total incoming energy $E_\cdot$ through the walls (in kWh), solar energy gains through the windows E_s (in kWh) and the incoming heat flux peak through the walls and windows $\Phi_{i,\cdot}^{max}$ (in Watts) in each of the 3 housing types (single-family, collective, hotel), for each of six PCMs and Air.

$$E_\cdot = A_t \times \left[(P_E \, e_\cdot^E + P_S \, e_\cdot^S + P_W \, e_\cdot^W + P_N \, e_\cdot^N + P_h \, e_\cdot^h \right) \tag{19}$$

$$E_s = A_t \times \left[W_{r,E} \, e_s^E + W_{r,S} \, e_s^S + W_{r,W} \, e_s^W + W_{r,N} \, e_s^N + W_{r,h} \, e_s^h \right] \tag{20}$$

$$\Phi_{i,\cdot}^{max} = A_t \times \left\{ \sup\left[\varphi_{i,\cdot}^{max,E}; \, \varphi_{i,\cdot}^{max,S} ; \, \varphi_{i,\cdot}^{max,W}; \, \varphi_{i,\cdot}^{max,N} ; \varphi_{i,\cdot}^{max,h} \right] \right\} \tag{21}$$

$$A^t = A^E + A^S + A^W + A^N + A^h \tag{22}$$

The energy savings $\Delta E(\%)$ and heat flux peak reduction $\Delta HF_i^{max}(\%)$ over the summer, where using PCMs is compared to no PCM can then be written as a percentage as follows:

$$\Delta E(\%) = 100 \times \frac{E_a - E_{pcm}}{E_a + E_s} \tag{23}$$

$$\Delta HF_i^{max}(\%) = 100 \times \frac{\Phi_a^{max} - \Phi_{pcm}^{max}}{\Phi_a^{max}} \tag{24}$$

The ΔE (%) and ΔHF_r (%) values are given in Fig.11 for Al Hoceima (a), Malaga (b), Taher(c) and Marseille (d), and in Fig.12 for Tripoli (e), Naples (f), Port Said (g) and Ankara (h).

- In terms of incoming heat flux peak reduction $\Delta HF_{i,max}$ (%),

    - PCM median melting temperatures of 22°C, 24°C, and 26°C lead to no reduction (negative) in both North and South Mediterranean climate family, except for Malaga (Spain) where a low reduction can be seen, not exceeding 10% for the hotel type (15 floors).

    - PCM median melting temperature of 28°C reduces the heat flux peak by up to 40% in the North Mediterranean climate family and leads to no reduction in the South Mediterranean family, except for Al Hoceima with 30%.

    - PCM median melting temperatures of both 30°C and 32°C are efficient for heat flux peak reduction in both climate families, except Tripoli (Libya); the 30°C value is efficient in Al Hoceima (Morocco), Marseille, Ankara (Turkey), and Port Said (Egypt), while 32°C is better in Malaga (Spain), Naples (Italy), and Taher (Algeria).

- In terms of energy savings ΔE (%):

    - PCM median melting temperatures of 22°C, 30°C and 32°C lead to inefficient or negative gains in both the North and South Mediterranean climate family.

    - Gains for a PCM median melting temperature of 24°C reach values of up to 8% for Al Hoceima (Morocco) and Marseille (France), 25% for Ankara (Turkey). For other cities, no energy savings were observed.

    - Gains for a PCM median melting temperature of 26°C reach 58%, 54%, 50%, 44%, 28%, 15% for Ankara (Turkey), Naples (Italy), Al Hoceima (Morocco), Malaga (Spain), Marseille (France), and Taher (Algeria), respectively, whereas in Tripoli (Libya), Port Said (Egypt) they are unfavorable.

    - For the PCM median melting temperature of 28°C, energy saving does not exceed 25% in Ankara, 10% in Al Hoceima and Marseille, while no energy savings were observed in the other cities.

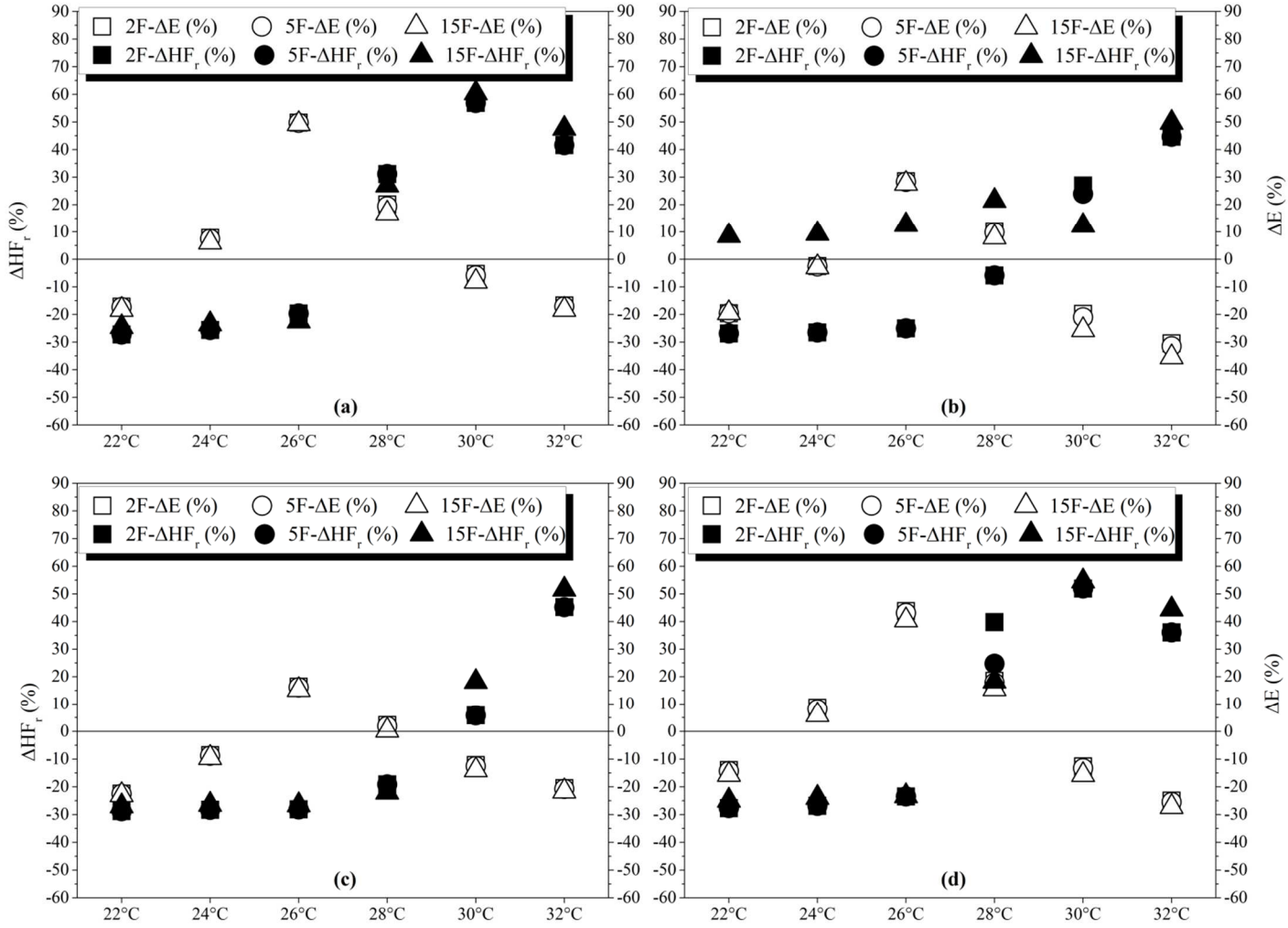

Figure 11. Energy savings and heat flux peak reduction in: (a) Al Hoceima, (b) Malaga, (c) Taher, (d) Marseille

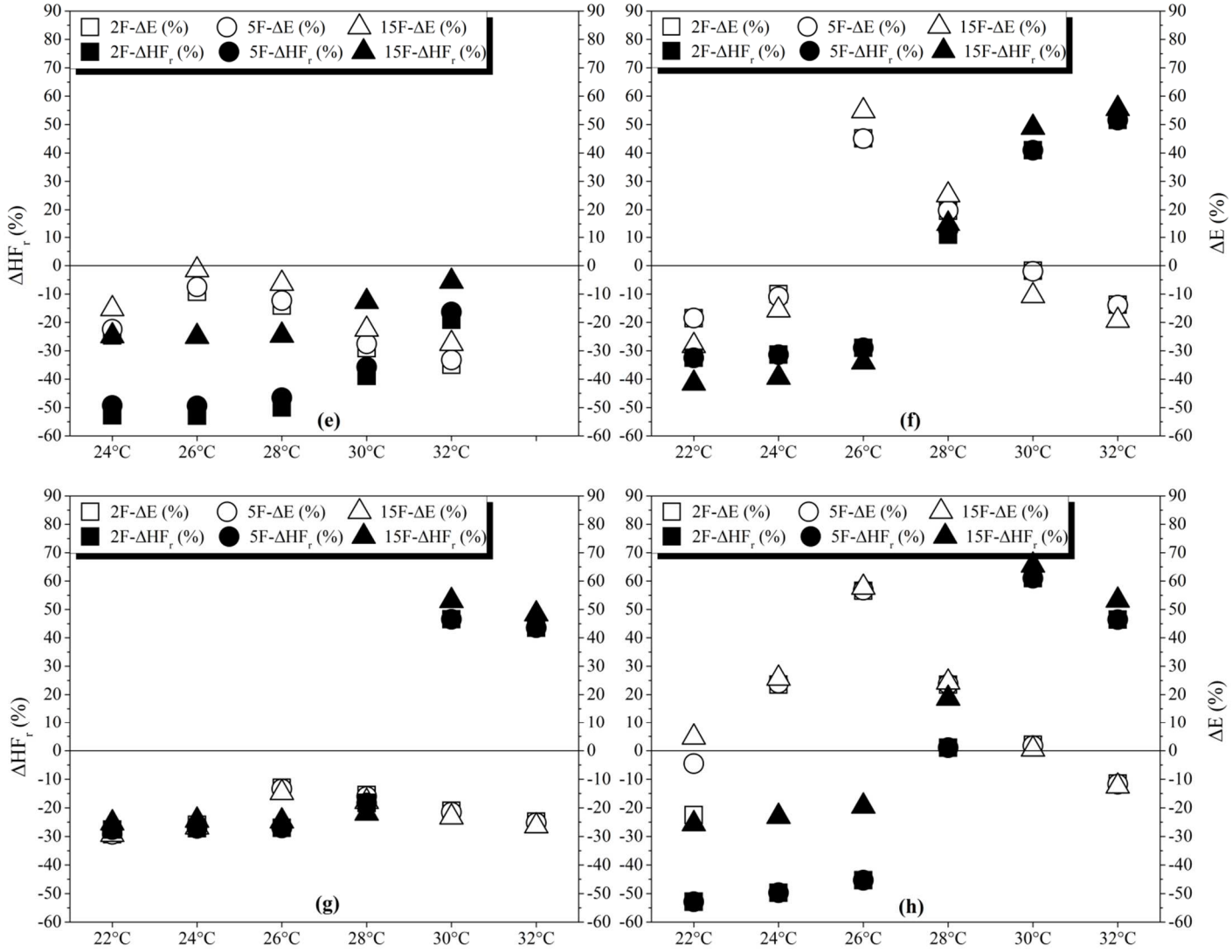

Figure 12. Energy savings and heat flux peak reduction in: (e) Tripoli, (f) Naples, (g) Port Said (h) Ankara

The preceding remarks encourage planning the use of PCMs with a median melting temperature of 26°C in new building constructions in both climates, except for Tripoli and Port Said, where no energy savings were observed. In addition, unlike the heat flux peak reduction, the energy savings depend less on the type of building. Thus, in the following sections we will consider an average value for the three typologies described in this study.

Using the PCM with T_m=26°C, we can see in Fig. 13 that the energy savings decrease from West to East in the South Mediterranean family. Summers in the West of this region are milder, with average temperatures at night not exceeding 21°C, due to the proximity of the Atlantic Ocean. This effectively regenerates the PCM overnight and provides significant energy savings. On the other hand, the East is influenced by the hot desert climate with hot summers and high night temperatures, which explains the poor performance of the PCM in Port Said and Tripoli. Unlike the South Mediterranean climate family, energy savings in the

North Mediterranean family increase from West to East. The Western part is characterized by a typical hot summer climate, a prevalent form of the Mediterranean climate, with high temperatures during the day in summer, and rapid cooling at night, which offers excellent conditions to benefit from the melting (during the day) and solidification (at night) of the PCM. As we move further East, the energy savings recorded using PCM 26°C are the most significant. Here, the summer becomes increasingly cold due to the proximity of the continental climate of Eastern Europe, which explains the excellent performance, even when using PCM with a melting temperature below 26°C (22°C for 15-floor buildings and 24°C for 2-, 5- and 15-floor buildings).

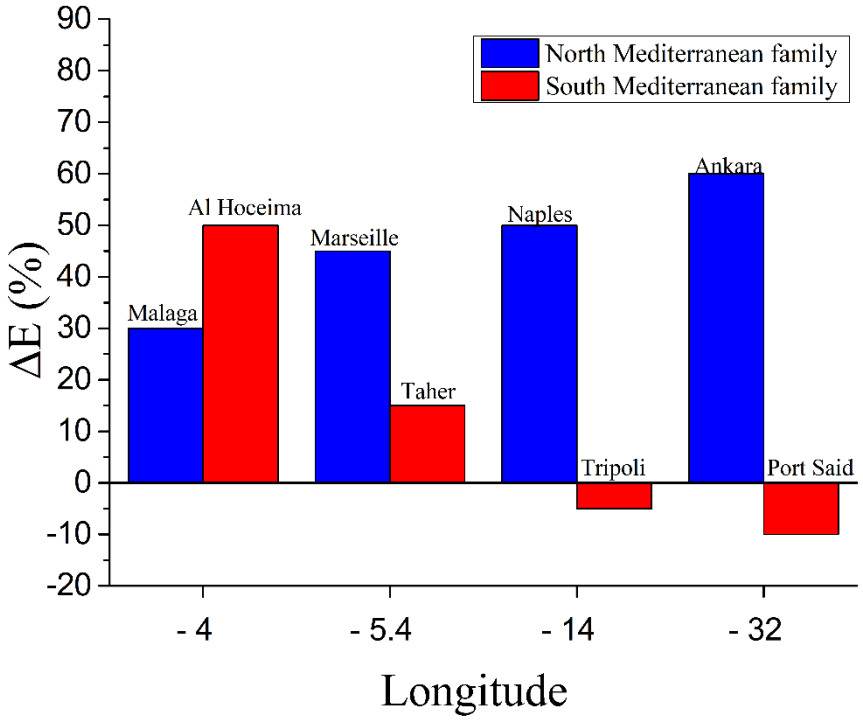

Figure 13. Energy savings in Northern and Southern Mediterranean cities using PCM with 26°C median melting temperature

3.4 Recommendation of PCM with T_m =26°C based on the Cooling Degree Day

In order to generalize the results obtained in this study and our previous studies [47], we propose to guide decision-making concerning the use (or not) of PCM with T_m=26°C based on the Cooling Degree Day (CDD) of the considered city. We would like to recall here that the results of the previous study recommend the use of PCMs with a median melting temperature close to 27°C. In order to validate our position under the same PCM conditions as the present study, we calculated the energy savings for the six cities in the previous study, this time using the PCM with T_m=26°C.

Figure 14 presents the energy savings as a function of the Cooling Degree Day (CDD) of fourteen cities: eight cities from the present study and six from our previous study [47]. The general shape of the scatter plot indicates an important relationship between energy savings and CDD. This relationship can be predicted using equation (25), which correlates energy savings to the CDD of a given location ($R^2 = 0.91$):

$$\Delta E\ (\%) = -0.1031\ \times \mathrm{CDD} + 74.819 \qquad (25)$$

The trend curve shows a negative correlation between these two parameters: energy savings decrease as the CDD increases. In addition, the intersection of the trend curve with the CDD axis demonstrates a limit in the effectiveness of PCMs; from a CDD near to 700, no energy savings could be achieved. The climatic conditions of the cities with a CDD above this value will not allow the regeneration of PCMs and therefore drastically reduce the interest of latent heat in improving the thermal performance of the building envelope.

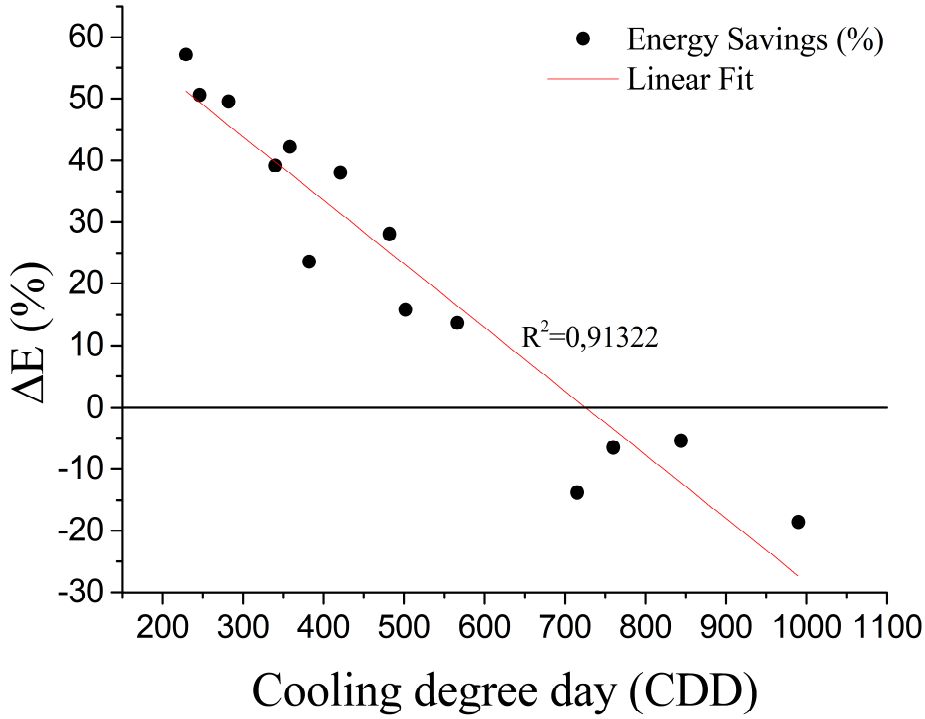

Figure 14. Energy savings using PCM with T_m=26°C as a function of the Cooling Degree Day (CDD) for 14 locations

Conclusions and recommendations

This research investigated the application of Phase Change Materials in building walls for East, South, West, North, and roof (horizontal) orientations in the Mediterranean region. The article deals with climatic conditions in 8 representative cities, which were grouped into two families, corresponding to two different thermal behaviors concerning heat flux density: South and North Mediterranean climate families.

Independently of the orientations, for a typical day (July 21), under both climate groups, the inside heat flux of the walls followed the external conditions when the PCM was entirely solid or liquid, and remained constant when the PCM was partially liquid or partially solid. However, the critical weather conditions during the nighttime for the South Mediterranean climate family imply a continual heat flux density inside the room, in contrast to the North Mediterranean climate family, where the ambient temperature was lower than the inside set point temperature value of 26°C.

To quantify the heat flux peak reduction and the energy savings achieved using our hollow bricks containing PCM, three typical dwellings were considered in the two climate families. The results proved that the PCMs with median melting temperatures of 28°C, 30°C and 32°C were efficient in reducing the heat flux peak in all housing types: single-family-housing (2 floors), collective-housing (5 floors), and hotel-housing (15 floors), in both climates, except in Port Said which is hugely affected by the desert climate.

Regarding energy savings, the PCM with 26°C median melting temperature can save up to 56% of the energy needed to maintain the internal comfort temperature at a 26°C set point temperature in the North-East Mediterranean climate and 50% in the South-West Mediterranean climate. It is therefore recommended that PCMs with a 26°C median melting temperature are used in new Mediterranean buildings to increase comfort and reduce cooling energy needs.

In order to guide the choice of the use of the recommended PCM, decision-makers can refer to the correlation established in this paper to evaluate energy savings based solely on the Cooling Degree Day. Finally, this first evaluation should be accompanied by an environmental and economic study looking into the savings in terms of cost and reduction of greenhouse gas emissions.

References

[1] S. V. Aleh Cherp, Adeola Adenikinju, Andreas Goldthau, Francisco Hernandez, Larry Hughes, Jaap Jansen, Jessica Jewell, Marina Olshanskaya, Ricardo Soares de Oliveira, Benjamin Sovacool, *Energy and security [3]*, vol. 23, no. 1. 2006.

[2] M. Lafrance and S. Esterly, "Launch of IEA's New Transition to Sustainable Buildings Strategies and Opportunities to 2050 Publication," no. June, pp. 1–23, 2013.

[3] I. Energy and S. Transformations, "Tracking Clean Energy Progress 2017 Tracking Clean Energy Progress 2017," 2017.

[4] R. Ford, M. Pritoni, A. Sanguinetti, and B. Karlin, "Categories and functionality of smart home technology for energy management," *Build. Environ.*, vol. 123, pp. 543–554, 2017, doi: 10.1016/j.buildenv.2017.07.020.

[5] Y. Hamidi, B. El Gharbi, H. Hafs, M. Malhaa, and A. Bah, "Numerical Study of Trombe Wall as a Passive Ventilation System: The Case of Moroccan Climate," Nov. 2019, doi: 10.1109/IRSEC48032.2019.9078162.

[6] S. S. Together, "The Future of Cooling :Opportunities for energy- efficient air conditioning," no. INTERNATIONAL ENERGY AGENCY, 2018.

[7] P. Alpert, S. O. Krichak, H. Shafir, D. Haim, and I. Osetinsky, "Climatic trends to extremes employing regional modeling and statistical interpretation over the E. Mediterranean," *Glob. Planet. Change*, vol. 63, no. 2–3, pp. 163–170, 2008, doi: 10.1016/j.gloplacha.2008.03.003.

[8] F. Kuznik, K. Johannes, and D. David, *Integrating phase change materials (PCMs) in thermal energy storage systems for buildings*. Woodhead Publishing Limited, 2014.

[9] M. Duquesne, C. Mailhé, K. Ruiz-Onofre, and F. Achchaq, "Biosourced organic materials for latent heat storage: An economic and eco-friendly alternative," *Energy*, vol. 188, 2019, doi: 10.1016/j.energy.2019.116067.

[10] F. S. Javadi, H. S. C. Metselaar, and P. Ganesan, "Performance improvement of solar thermal systems integrated with phase change materials (PCM), a review," *Sol. Energy*, vol. 206, no. April, pp. 330–352, 2020, doi: 10.1016/j.solener.2020.05.106.

[11] G. Fang, S. Wu, and X. Liu, "Experimental study on cool storage air-conditioning system with spherical capsules packed bed," *Energy Build.*, vol. 42, no. 7, pp. 1056–1062, 2010, doi: 10.1016/j.enbuild.2010.01.018.

[12] A. Dugué, S. Raji, P. Bonnamy, and D. Bruneau, "E2VENT: An Energy Efficient Ventilated Façade Retrofitting System. Presentation of the Embedded LHTES System," *Procedia Environ. Sci.*, vol. 38, pp. 121–129, 2017, doi: 10.1016/j.proenv.2017.03.093.

[13] Z. Liu *et al.*, "A review on macro-encapsulated phase change material for building envelope applications," *Build. Environ.*, vol. 144, no. April, pp. 281–294, 2018, doi: 10.1016/j.buildenv.2018.08.030.

[14] F. Souayfane, F. Fardoun, and P. Biwole, "Phase Change Materials (PCM) for cooling applications in buildings : A review," *Energy Build.*, 2016, doi: 10.1016/j.enbuild.2016.04.006.

[15] S. Raquel, J. Luís, and B. De Aguiar, “Phase change materials and energy e ffi ciency of buildings : A review of knowledge,” vol. 27, no. September 2019, 2020, doi: 10.1016/j.est.2019.101083.

[16] S. Ručevskis, P. Akishin, and A. Korjakins, “Parametric analysis and design optimisation of PCM thermal energy storage system for space cooling of buildings,” *Energy Build.*, vol. 224, 2020, doi: 10.1016/j.enbuild.2020.110288.

[17] B. Maleki, A. Khadang, H. Maddah, M. Alizadeh, A. Kazemian, and H. M. Ali, “Development and thermal performance of nanoencapsulated PCM/ plaster wallboard for thermal energy storage in buildings,” *J. Build. Eng.*, vol. 32, no. July, p. 101727, 2020, doi: 10.1016/j.jobe.2020.101727.

[18] S. Kenzhekhanov, S. A. Memon, and I. Adilkhanova, “Quantitative evaluation of thermal performance and energy saving potential of the building integrated with PCM in a subarctic climate,” *Energy*, vol. 192, p. 116607, 2020, doi: 10.1016/j.energy.2019.116607.

[19] G. Gholamibozanjani and M. Farid, “Application of an active PCM storage system into a building for heating/cooling load reduction,” *Energy*, vol. 210, p. 118572, 2020, doi: 10.1016/j.energy.2020.118572.

[20] P. K. S. Rathore and S. K. Shukla, “An experimental evaluation of thermal behavior of the building envelope using macroencapsulated PCM for energy savings,” *Renew. Energy*, vol. 149, pp. 1300–1313, 2020, doi: 10.1016/j.renene.2019.10.130.

[21] R. Saxena, D. Rakshit, and S. C. Kaushik, “Experimental assessment of Phase Change Material (PCM) embedded bricks for passive conditioning in buildings,” *Renew. Energy*, vol. 149, pp. 587–599, 2020, doi: 10.1016/j.renene.2019.12.081.

[22] M. Arıcı, F. Bilgin, S. Nižetić, and H. Karabay, “PCM integrated to external building walls: An optimization study on maximum activation of latent heat,” *Appl. Therm. Eng.*, vol. 165, no. October 2019, 2020, doi: 10.1016/j.applthermaleng.2019.114560.

[23] E. Tunçbilek, M. Arıcı, M. Krajčík, S. Nižetić, and H. Karabay, “Thermal performance based optimization of an office wall containing PCM under intermittent cooling operation,” *Appl. Therm. Eng.*, vol. 179, no. July, 2020, doi: 10.1016/j.applthermaleng.2020.115750.

[24] D. K. Bhamare, M. K. Rathod, and J. Banerjee, “Numerical model for evaluating thermal performance of residential building roof integrated with inclined phase change material (PCM) layer,” *J. Build. Eng.*, vol. 28, no. October 2019, 2020, doi: 10.1016/j.jobe.2019.101018.

[25] L. F. Cabeza *et al.*, “Behaviour of a concrete wall containing micro-encapsulated PCM after a decade of its construction,” *Sol. Energy*, vol. 200, no. October, pp. 108–113, 2020, doi: 10.1016/j.solener.2019.12.003.

[26] C. R. Yu, H. Sen Guo, Q. C. Wang, and R. D. Chang, “Revealing the impacts of passive cooling techniques on building energy performance: A residential case in Hong Kong,” *Appl. Sci.*, vol. 10, no. 12, 2020, doi: 10.3390/APP10124188.

[27] R. F. J. Š. J. K. J. Černý, “Energy Efficiency of Novel Interior Surface Layer with Improved Thermal Characteristics and Its E ff ect on Hygrothermal Performance of

Contemporary," *Energies*, 2020.

[28] S. Lu, B. Liang, X. Li, X. Kong, W. Jia, and L. Wang, "Performance analysis of PCM ceiling coupling with earth-air heat exchanger for building cooling," *Materials (Basel).*, vol. 13, no. 13, pp. 1–17, 2020, doi: 10.3390/ma13132890.

[29] L. F. Cabeza, C. Castellón, M. Nogués, M. Medrano, R. Leppers, and O. Zubillaga, "Use of microencapsulated PCM in concrete walls for energy savings," *Energy Build.*, vol. 39, no. 2, pp. 113–119, 2007, doi: 10.1016/j.enbuild.2006.03.030.

[30] A. Castell, I. Martorell, M. Medrano, G. Pérez, and L. F. Cabeza, "Experimental study of using PCM in brick constructive solutions for passive cooling," *Energy Build.*, vol. 42, no. 4, pp. 534–540, 2010, doi: 10.1016/j.enbuild.2009.10.022.

[31] R. Saxena, D. Rakshit, and S. C. Kaushik, "Phase change material (PCM) incorporated bricks for energy conservation in composite climate : A sustainable building solution," *Sol. Energy*, vol. 183, no. January, pp. 276–284, 2019, doi: 10.1016/j.solener.2019.03.035.

[32] L. Shilei, Z. Neng, and F. Guohui, "Impact of phase change wall room on indoor thermal environment in winter," vol. 38, pp. 18–24, 2006, doi: 10.1016/j.enbuild.2005.02.007.

[33] L. Shilei, F. Guohui, Z. Neng, and D. Li, "Experimental study and evaluation of latent heat storage in phase change materials wallboards," vol. 39, pp. 1088–1091, 2007, doi: 10.1016/j.enbuild.2006.11.012.

[34] K. Darkwa, P. W. O. Õ. Callaghan, and D. Tetlow, "APPLIED Phase-change drywalls in a passive-solar building," vol. 83, pp. 425–435, 2006, doi: 10.1016/j.apenergy.2005.05.001.

[35] P. W. Griffiths and P. C. Eames, "Performance of chilled ceiling panels using phase change material slurries as the heat transport medium," vol. 27, pp. 1756–1760, 2007, doi: 10.1016/j.applthermaleng.2006.07.009.

[36] G. Zhou, Y. Zhang, Q. Zhang, K. Lin, and H. Di, "APPLIED Performance of a hybrid heating system with thermal storage using shape-stabilized phase-change material plates," vol. 84, pp. 1068–1077, 2007, doi: 10.1016/j.apenergy.2006.09.015.

[37] A. Pasupathy, L. Athanasius, and R. Velraj, "Experimental investigation and numerical simulation analysis on the thermal performance of a building roof incorporating phase change material (PCM) for thermal management," vol. 28, pp. 556–565, 2008, doi: 10.1016/j.applthermaleng.2007.04.016.

[38] R. Barzin, J. J. J. Chen, B. R. Young, and M. M. Farid, "Application of PCM energy storage in combination with night ventilation for space cooling," *Appl. Energy*, vol. 158, pp. 412–421, 2015, doi: 10.1016/j.apenergy.2015.08.088.

[39] W. Lin, Z. Ma, M. I. Sohel, and P. Cooper, "Development and evaluation of a ceiling ventilation system enhanced by solar photovoltaic thermal collectors and phase change materials," *ENERGY Convers. Manag.*, vol. 88, pp. 218–230, 2014, doi: 10.1016/j.enconman.2014.08.019.

[40] M. Jaworski, P. Łapka, and P. Furman, "Numerical modelling and experimental studies of thermal behaviour of building integrated thermal energy storage unit in a form of a

ceiling panel," vol. 113, pp. 548–557, 2014, doi: 10.1016/j.apenergy.2013.07.068.

[41] H. M. Chou, C. R. Chen, and V. L. Nguyen, "A new design of metal-sheet cool roof using PCM," *Energy Build.*, vol. 57, pp. 42–50, 2013, doi: 10.1016/j.enbuild.2012.10.030.

[42] X. Jin, M. A. Medina, and X. Zhang, "On the importance of the location of PCMs in building walls for enhanced thermal performance," *Appl. Energy*, vol. 106, pp. 72–78, Jun. 2013, doi: 10.1016/j.apenergy.2012.12.079.

[43] S. Lu, B. Xu, and X. Tang, "Experimental study on double pipe PCM fl oor heating system under different operation strategies," *Renew. Energy*, vol. 145, pp. 1280–1291, 2020, doi: 10.1016/j.renene.2019.06.086.

[44] K. Lin, Y. Zhang, X. Xu, and H. Di, "Experimental study of under-floor electric heating system with shape-stabilized PCM plates," vol. 37, pp. 215–220, 2005, doi: 10.1016/j.enbuild.2004.06.017.

[45] K. Nagano, S. Takeda, T. Mochida, K. Shimakura, and T. Nakamura, "Study of a floor supply air conditioning system using granular phase change material to augment building mass thermal storage — Heat response in small scale experiments," vol. 38, pp. 436–446, 2006, doi: 10.1016/j.enbuild.2005.07.010.

[46] A. G. Entrop, H. J. H. Brouwers, and A. H. M. E. Reinders, "Experimental research on the use of micro-encapsulated Phase Change Materials to store solar energy in concrete floors and to save energy in Dutch houses," *Sol. Energy*, vol. 85, no. 5, pp. 1007–1020, 2011, doi: 10.1016/j.solener.2011.02.017.

[47] Z. Aketouane *et al.*, "Energy savings potential by integrating Phase Change Material into hollow bricks: The case of Moroccan buildings," *Build. Simul.*, vol. 11, no. 6, pp. 1109–1122, 2018, doi: 10.1007/s12273-018-0457-5.

[48] R. Vicente and T. Silva, "Brick masonry walls with PCM macrocapsules: An experimental approach," *Appl. Therm. Eng.*, vol. 67, no. 1–2, pp. 24–34, 2014, doi: 10.1016/j.applthermaleng.2014.02.069.

[49] N. Hichem, S. Noureddine, S. Nadia, and D. Djamila, "Experimental and numerical study of a usual brick filled with PCM to improve the thermal inertia of buildings," *Energy Procedia*, vol. 36, pp. 766–775, 2013, doi: 10.1016/j.egypro.2013.07.089.

[50] "RUBITHERM® RT-PCM RT-LINE," *Rubitherm Technologies GmbH*, 2019. https://www.rubitherm.eu.

[51] T. G. Chuah, D. Rozanna, A. Salmiah, S. Y. Thomas Choong, and M. Sa'ari, "Fatty acids used as phase change materials (PCMs) for thermal energy storage in building material applications," *Appl. Energy*, no. July, pp. 123–137, 2006.

[52] C. AB, "COMSOL Multiphysics®," 2020. www.comsol.com.

[53] Comsol, "Heat Transfer Module," pp. 1–222, 2015.

[54] A. M. Thiele, G. Sant, and L. Pilon, "Diurnal thermal analysis of microencapsulated PCM-concrete composite walls," *Energy Convers. Manag.*, vol. 93, pp. 215–227, 2015, doi: 10.1016/j.enconman.2014.12.078.

[55] N. P. Sharifi, G. E. Freeman, and A. R. Sakulich, “Using COMSOL modeling to investigate the efficiency of PCMs at modifying temperature changes in cementitious materials - Case study,” *Constr. Build. Mater.*, vol. 101, no. December, pp. 965–974, 2015, doi: 10.1016/j.conbuildmat.2015.10.162.

[56] J. Yu, C. Yang, and L. Tian, “Low-energy envelope design of residential building in hot summer and cold winter zone in China,” *Energy Build.*, vol. 40, no. 8, pp. 1536–1546, 2008, doi: 10.1016/j.enbuild.2008.02.020.

[57] ISO 6946, “Building components and building elements - Thermal resistance and thermal transmittance- Calculation method,” vol. 0, 1996, doi: 10.1111/j.1875-595X.2011.00062.x.

[58] M. C. Peel, B. L. Finlayson, and T. A. McMahon, “Updated world map of the Köppen-Geiger climate classification,” *Hydrol. Earth Syst. Sci.*, vol. 11, no. 5, pp. 1633–1644, Oct. 2007, doi: 10.5194/hess-11-1633-2007.